Atmospheric Environment 43 (2009) 1051–1058

Contents lists available at ScienceDirect

Atmospheric Environment

journal homepage: www.elsevier.com/locate/atmosenv

Methanesulphonic acid (MSA) stratigraphy from a Talos Dome ice core as a tool in depicting sea ice changes and southern atmospheric circulation over the previous 140 years

Silvia Becagli [a,*], Emiliano Castellano [a], Omar Cerri [a], Mark Curran [b], Massimo Frezzotti [c], Federica Marino [a,d], Andrea Morganti [a], Marco Proposito [c], Mirko Severi [a], Rita Traversi [a], Roberto Udisti [a]

[a] Department of Chemistry, University of Florence, Scientific Pole, via della Lastruccia, 3 Sesto F.no, I-50019, Florence, Italy
[b] Australian Antarctic Division and Antarctic Climate and Ecosystem CRC, Hobart, Tasmania 7001, Australia
[c] ENEA C.R. Casaccia, PO 2400, I-00100 Roma, Italy
[d] DISAT, University of Milano-Bicocca, Piazzale della Scienza 1, I-20126 Milano, Italy

ARTICLE INFO

Article history:
Received 24 June 2008
Received in revised form
22 October 2008
Accepted 13 November 2008

Keywords:
Methanesulphonic acid
Ice core
Sea ice
SOI
SAM
Antarctica
Talos Dome

ABSTRACT

Firn core methanesulphonic acid (MSA) stratigraphy from Talos Dome (East Antarctica) was compared with anomalies of the satellite-measured sea ice extent (1973–1995) in the Ross Sea and Wilkes Land oceanic sector. In spite of the sparseness of sea ice data, the MSA maxima fit with many positive sea ice anomalies in the Ross Sea. This evidence suggests that marine biogenic activity enhanced by large sea ice cover is an important, but not exclusive, factor in controlling MSA concentration in snow precipitation at Talos Dome. Other than source intensity, differences in regional atmospheric transport mechanisms affect the arrival of MSA-rich aerosol at Talos Dome. To clarify the role of transport processes in bringing biogenic aerosol to Talos Dome, a spectral analysis was applied to the MSA, SOI (South Oscillation Index), and SAM (Southern Annular Mode) record. Synchronicity or phase shift between the chemical signature and atmospheric circulation modes were tested. The variations in the MSA profile have a periodicity of 6.9, 4.9, 3.5, and 2.9 years. The 6.9 and 2.9 year periodicities show a strong positive correlation and are synchronous with corresponding SOI periodicity. This variability could be related to an increase in MSA source intensity (by dimethylsulphide from phytoplanktonic activity) linked to the sea ice extent in the Ross Sea area, but also to an increased strength in transport processes. Both of these factors are correlated with La Niña events (SOI positive values). Furthermore, SAM positive values are related to an increased sea ice extent in the Ross Sea sector and show two main periodicities 3.3 and 3.8 years. These periodicities determine the MSA variability at 3.5 years. However, the effect of intensification of the polar vortex and the consequent reduction in transport process intensity, which reduce the delivery of air masses enriched in MSA from oceanic areas to Talos Dome, make the effect of the SAM on the MSA concentration at Talos Dome less active than the SOI. In this way, snow deposition at the Talos Dome records larger MSA concentration by the combined effects of increased source emissions and more efficient transport processes. The MSA record from Talos Dome can therefore be considered a reliable proxy of sea ice extent when the effect of changes in transport processes in this region of Antarctica is considered. Over the previous 140 years, these conditions occur with a periodicity of 6.9 years.

1. Introduction

The interaction between oceanic biogenic productivity and global climate is one of the most intriguing and controversial aspects in understanding the complex relationship between climate forcing and environmental feedback. Changes in phytoplanktonic activity are influenced by variations in solar irradiance, Sea Surface Temperature (SST), and nutrient availability. Oceanic biota metabolic processes are likely to affect climate through direct and indirect effects (Charlson et al., 1987; Andreae and Crutzen, 1997). These effects are due to biogenic aerosol production and can be influenced by changes in cloud coverage (in turn, affecting albedo and the hydrological cycle), uptake of CO_2 at the atmosphere–seawater interface, CO_2 storing via oceanic biological pump, and CH_4 emission. In this way, changes in phytoplanktonic productivity caused by external forcing, such as variations in oceanic and atmospheric circulation, sea ice extent and nutrients or oligo-element supply (from changes in up welling areas or

* Corresponding author. Tel.: +39 055 4573350; fax: +39 055 4573385.
E-mail address: silvia.becagli@unifi.it (S. Becagli).

1352-2310/$ – see front matter © 2008 Elsevier Ltd. All rights reserved.
doi:10.1016/j.atmosenv.2008.11.015

continental dust deposition on the seawater surface), can exert positive or negative feedback, which can amplify or mitigate climate changes on a regional or global scale.

While the climate–ocean relationship is generally recognised in a qualitative sense, the quantitative estimation of the contribution of oceanic biogenic activity to climate tuning at present and in the past is still under discussion. The sulphur-cycle compounds emitted into the atmosphere by algal metabolic processes are assumed to constitute the most effective source of Cloud Condensation Nuclei (CCN) in remote oceanic regions, although it is now recognised that many other non-sulphuric marine biotic compounds can affect CCN formation in the atmosphere (Meskhidze and Nenes, 2006). Gaseous dimethylsulphide emitted into the atmosphere is oxidised into H_2SO_4 and methanesulphonic acid (MSA) (Gondwe et al., 2003 and references therein). A large Henry constant, which defines the affinity toward atmospheric moisture, results in a highly efficient gas-to-particle conversion processes making these compounds the dominant source of sub-micrometric secondary aerosol in remote marine regions (Brimblecombe, 1996).

Antarctica is encircled by a highly biologically productive ocean and is a major site for the production of the cold and deep water that drives ocean circulation. Antarctica is also a major participant in the Earth's albedo dynamics and is an important driving component for atmospheric circulation. For these reasons, ice core stratigraphies of oceanic biogenic markers (mainly sulphate and methanesulphonate) have been used in reconstructing cause and effect relationships between climate forcing and environmental feedback in the past. While a general picture is now widely accepted, specific features of these interactions are still poorly understood. This is mainly due to uncertainties in the reliability of biogenic marker stratigraphies measured along ice cores for recording past changes in phytoplanktonic activity (Saigne and Legrand, 1987; Wolff et al., 2006). Indeed, sulphate is produced by several other sources, such as sea spray, continental dust, and volcanic emissions. Additionally, MSA, which only arises from the oxidation of biogenic DMS (e.g. Gondwe et al., 2003), is affected by post-depositional processes in the snow layers (Curran et al., 2002; Legrand et al., 1996; de Angelis and Legrand, 1995; Wagnon et al., 1999). Therefore, changes in the MSA stratigraphies that were previously attributed to variation in oceanic productivity (Legrand et al., 1991) were really caused by changes in snow accumulation rates, snow acidity, and atmospheric load of dust particles (able to fix MSA as non-volatile salts). More recent evidence from high-resolution stratigraphies of sulphate and MSA fluxes along the ice core drilled at Dome C (East Antarctica), in the framework of the European Project for Ice Coring in Antarctica (EPICA), revealed that oceanic productivity was not significantly changed during glacial and interglacial periods (Wolff et al., 2006). This result weakened the generally accepted consideration that higher phytoplanktonic growth (by atmospheric deposition of oligo-elements) in High-Nutrient Low-Chlorophyll (HNLC) oceanic areas was a common feature in cold climatic stages and could have exerted a powerful feedback on the climate during glacial inceptions or terminations (Röthlisberger et al., 2004 and references therein).

Furthermore, the relationship between DMS production (and, by extension, the MSA concentration in the snow deposition) and regional meteorological conditions (SST, atmospheric circulation modes, and sea ice) is still controversial.

On one side, changes in MSA deposition in Antarctica could be attributed to a higher phytoplanktonic activity (i.e., larger DMS emission into the atmosphere) primed by larger sea ice extent. It is important to note that the capability of reconstructing past sea ice extension from ice core stratigraphy deserves increasing attention due to the relevant and complex role played by sea ice in the climate system. Sea ice affects the salinity through freezing and melting processes and temperature via albedo of superficial seawater, thereby influencing Antarctic bottom water formation and global ocean circulation (Keeling and Stephens, 2001). The ice cover also limits the atmosphere/seawater exchange of CO_2, which affects the positive feedback of this greenhouse gas on the climate, especially during periods of glaciation and deglaciation (Stephens and Keeling, 2000).

On the other hand, changes in the efficiency of transport processes, which transports marine air masses toward the internal areas of the continent (hemispheric and regional circulation modes), could rule MSA deposition on coastal and inner areas of the continent.

To clarify these aspects, MSA stratigraphies from ice cores drilled in Antarctic coastal sites, where the snow accumulation rate is sufficient enough to preserve its annual record, have to be compared with contemporaneous changes in sea ice extent and the atmospheric circulation mode. This knowledge is crucial in order to reliably interpret the MSA stratigraphies from the past.

In this paper, the periodicity in the MSA stratigraphy from Talos Dome (Northern Victoria Land, East Antarctica), Antarctic Circumpolar Wave (ACW) (e.g. White and Tourre, 2003 and references therein), SOI (e.g. Turner, 2004 and references therein), and Antarctic Oscillation or Southern Annular Mode (AAO or SAM) (e.g. Hall and Visbeck, 2002; Thompson and Solomon, 2002) were compared with the aim of understanding how the most effective atmospheric circulation modes in Antarctica can affect MSA snow deposition at Talos Dome. This information will be used to reconstruct changes in sea ice extent and atmospheric circulation modes from stratigraphies of a deep ice core (about 1600 m depth) now being carried out at the same site by the TALDICE project that is assumed to cover all of the previous glacial–interglacial cycle.

2. Data and methods

2.1. Drilling site

Talos Dome (72°48′S, 159°06′E; 2316 m a.s.l.; 290 and 250 km from the Pacific and Ross Sea coasts, respectively) is a coastal dome in Northern Victoria Land on the edge of the East Antarctic ice sheet (Fig. 1). It is located on the ice divide between accumulation basins

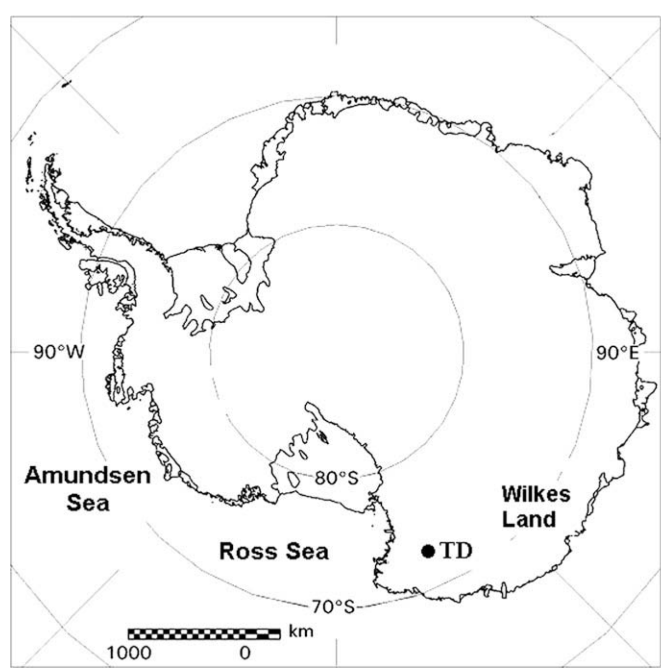

Fig. 1. Schematic map of Antarctica with an indication of the drilling site (TD).

facing the Pacific Ocean and Ross Sea sectors and ice core stratigraphies from this site are expected to provide information about environmental and climatic changes in the surrounding oceans.

Airborne radar measurements show a flat snow layering with the bedrock at about 400 m in elevation covered by about 1900 m of ice (Frezzotti et al., 2004). The surface strain network showed a mean accumulation rate of 83 $kg\,m^{-2}\,yr^{-1}$ with a standard deviation of 15 $kg\,m^{-2}\,yr^{-1}$ for the period 1996–2002 (Frezzotti et al., 2004). This averaged accumulation rate is in accordance with the values of 80 $kg\,m^{-2}\,yr^{-1}$ that were determined for a Talos Dome firn core (TD96) over the previous 800 years (Stenni et al., 2002). Unperturbed stratigraphy and high ice thickness make Talos Dome a promising site for deep ice coring, which started in December 2004 and reached a depth of 1619.2 m, which is a few meters above the bedrock, in December 2007. The ice core record is assumed to cover the previous 120 kyr. In preparation of the deep drilling, an 89 m firn core (TD96) was drilled at the dome culmination in November 1996 and, in this work, the results obtained from this firn core are reported.

2.2. Analytical methods

After retrieval, the firn core sections were kept frozen ($-20\,°C$) and shipped to Italy where they were sub-sampled with a resolution of about 3 cm in a cold room under a class 100 laminar flow hood and analysed just after melting for sulphur species (MSA and SO_4^{2-}) and other ionic components (Cl^-, NO_3^-, F^-, Na^+, NH_4^+, K^+, Mg^{2+} and Ca^{2+}) by ion chromatography (Morganti et al., 2007).

Sea-salt-sulphate ($ssSO_4^{2-}$) was calculated from the Na^+ content using the SO_4^{2-}/Na^+ ratio in bulk seawater (0.253 w/w), this contribution was subtracted from total SO_4^{2-} for non-sea-salt-sulphate ($nssSO_4^{2-}$) calculation. Rankin et al. (2002) suggested that the formation of frost flowers on fresh sea ice was one of the main sources of sea spray for Antarctic coastal regions. This aerosol is depleted SO_4^{2-} due to the precipitation of mirabilite ($Na_2SO_4 \cdot 10H_2O$) at temperatures below $-8.2\,°C$ during the frost flower formation therefore a lower SO_4^{2-}/Na^+ ratio is proposed for $nssSO_4^{2-}$ calculation. Since sea spray aerosol from frost flowers in Northern Victoria Land seems to be evident only in sporadic precipitation events (Benassai et al., 2005) and its contribution to the global budget of annual $ssSO_4^{2-}$ deposition at Talos Dome is not quantifiable, a SO_4^{2-}/Na^+ ratio of 0.253 was assumed in calculating the $nssSO_4^{2-}$ fraction.

2.3. Firn core dating

The firn core stratigraphic dating was performed by using chemical markers with a well defined seasonal pattern ($nssSO_4^{2-}$ for the whole firn core and stable isotopes and H_2O_2 for the more superficial snow layers) coupled with observation of dated reference horizons (Stenni et al., 2002; Becagli et al., 2004). The tie points are known volcanic eruptions revealed by high concentration peaks (exceeding the background plus twice the standard deviation) in the $nssSO_4^{2-}$ profile and tritium peaks from the 1960s. The dating error is due to incorrect identification or a lack of a $nssSO_4^{2-}$ seasonal signal and is, at the worst, ±5 years in points that are far from dated volcanic peak along the whole firn core (Stenni et al., 2002). Over the top 23 m of the firn core, the estimated dating error is one year because of the high occurrence of known reference horizons.

2.4. Statistical methods

Spectral analysis is a powerful tool in highlighting periodicities in chemical temporal profiles likely reflecting major changes in climatic and environmental conditions. Periodogram plots shown in this paper were computed by using STATISTICA® software (by Stat Soft) accomplished with a Fast Fourier Transform (FFT) algorithm. This mathematical tool can identify characteristic frequencies in temporal variations of a selected marker by using trigonometric functions to fit the temporal profiles. In this way, uncertainty in the dating of some snow layers decreases the significance of the determined periodicities (broader peaks in the periodogram plot); however, this loss of significance is counterbalanced by the large data set.

The software requires constant time resolution of the compared time series. Since reliable data exist for MSA with an annual resolution (see below), SOI and SAM time series, even if available and reliable at higher resolutions, were yearly averaged.

In order to discriminate main periodicities, a spectral density was computed. Spectral density is the frequency region consisting of many adjacent frequencies that contribute most to the overall periodic behaviour of the series. Spectral density is obtained by smoothing the periodogram values via a Tukey–Hamming window (Blackman and Tukey, 1958), which is a weighted moving average. Furthermore, a red noise function (noise increasing as frequency decreases – Ghil et al., 2002) and 90%, 95%, and 99% confidence level curve (Mann and Lees, 1996) tests were performed on the spectral density values in order to determine highly significant frequencies. The red noise function is preferred over the simple white noise (constant noise value at every frequency) because it better represents the frequency spectrum of a climatic and geophysical time series when no significant periodicity occurs. Parameters changing in a non-periodical way also show higher periodogram values at lower frequencies (Hasselmann, 1976; Mitchell, 1976).

SOI and sea ice anomalies in the Ross and Wilkes sector data were downloaded from the National Oceanic and Atmospheric Administration (NOAA) via the National Snow and Ice Data Centre (NSIDC) web site (http://nsidc.org/data). The SAM annual mean data set from 1957 was obtained from http://jisao.washington.edu.

2.5. MSA stratigraphy reliability

In paleo-climatic and paleo-environmental studies, changes in ice core stratigraphies can be attributed to variations in source intensity or transport efficiency of atmospheric gases and aerosols only if chemical markers are irreversibly fixed in the snow layer, and thus reflecting the original atmospheric composition. For components that are deposited as, or can transform into, volatile species, like chloride, nitrate and MSA, post-depositional processes (diffusion, migration, and re-emission into the atmosphere) become important in sites where accumulation of snow is low (Curran et al., 2002; Wagnon et al., 1999). It is generally assumed (Pasteur and Mulvaney, 2000; Curran et al., 2002) that MSA migrates in the snow pack through diffusion of the acidic species in a liquid or vapour phase. Such migration stops in the winter layers where it is neutralised or made alkaline and the MSA forms stable salts.

Fig. 2 shows the MSA and $nssSO_4^{2-}$ profiles over the first 23 m of the TD96 firn core, covering approximately the previous 140 years, as a common record of biogenic aerosol deposition. The smoothing effect exerted by the annual mean calculation over the entire depth interval is more evident for $nssSO_4^{2-}$ than for MSA. Indeed, $nssSO_4^{2-}$ is irreversibly fixed in the snow layers and it is not affected by any post-depositional movement. On the contrary, the MSA averaged profile (dark line in Fig. 2) shows a similar trend to the high-resolution data (grey line in the plot) as depth increases. This evidence shows that the relatively high accumulation at Talos Dome ensures the preservation of the MSA record in the snow layers, but some summer–winter re-distribution of the original deposition may occur due to migration processes. Such seasonal smoothing makes the interpretation of the ice core MSA record at sub-annual

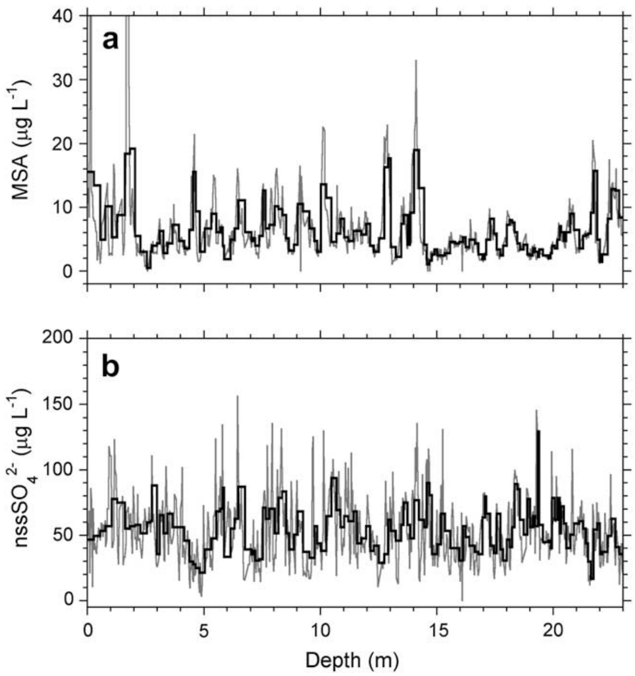

Fig. 2. MSA (a) and $nssSO_4^{2-}$ (b) profiles for the 23 m depth of the TD96 firn core corresponding to approximately 140 years. In both plots the grey lines indicate high-resolution data (measured concentration) and the bold dark lines represent the annual mean values.

resolution a very difficult task, but does not significantly affect the annual mean calculations. In this way, we use the MSA annual-averaged concentration in the TD96 firn core for comparison with changes in sea ice extent and atmospheric circulation modes (SOI, SAM).

3. Results and discussion

Changes in the MSA record over the previous 140 years from the Talos Dome ice core are interpreted in this work as an answer to variations of climatic (sea ice extent, SOI, and SAM) parameters through a comparison of their characteristic frequencies determined by spectral analysis. Although the Talos Dome ice core record covers the last 800 years, we discuss the trends observed over approximately the previous 140 years (from 1860 to 1996 AD), because SOI data are only available for this period.

3.1. Sea ice extent

Several studies have focused on finding a reliable relationship between MSA records from Arctic and Antarctic ice cores and changes in the sea ice extent. Positive correlations were found in ice cores drilled in Antarctica (Welch et al., 1993; Curran et al., 2003) and in Greenland ice cores (Legrand et al., 1997; Whung et al., 1994). In contrast, negative correlations were found in ice core stratigraphies from the Antarctic Peninsula (Pasteur et al., 1995) and from the Svalbard Islands (O'Dwyer et al., 2000). Both positive and negative correlations were found by Abram et al. (2007) around West Antarctica. The connection between sea ice and biogenic productivity is thought to occur through two main mechanisms: first, summer melting of sea ice discharges a large amount of micronutrients deposited on the sea ice surface by atmospheric scavenging that concentrate in the upper 30 m of the seawater (especially Fe, that reaches concentration as high as 2 mM – Sedwick and DiTullio, 1997) and priming phytoplankton blooms. Second, higher sea ice production reflects lower winter temperatures and higher biogenic production of dimethylsulphoniopropionate (DMSP), a precursor of MSA. In fact, algal cells (especially dinoflagellates and coccolithophorides; Stefels, 2000) protect themselves against salinity and low temperatures by producing intracellular DMSP, which is an osmolyte (Vairavamurthy et al., 1985), a cryoprotectant (Malin et al., 1992). DMSP is excreted from cells when salinity decreases for sea ice melting and in seawater it forms volatile DMS, which is emitted into the atmosphere where it is oxidised into MSA. Both these mechanisms agree with the result found by Gabric et al. (2005) that the sulphur species precursor of MSA are produced over the sea ice zone in austral spring as sea ice melts. Curran et al. (2003) demonstrated a close relationship between sea ice extent and MSA snow deposition and used its record from the Law Dome ice core (Wilkes Land, East Antarctica) to reconstruct the sea ice extent in the 80° E–140° E sector since 1840 A.D.

Fig. 3 shows the anomalies in sea ice extent recorded with weekly resolution from 1972 to 1995 in the Ross Sea and in the Pacific Ocean regions facing Wilkes Land. These marine sectors are assumed to be the dominant source areas for biogenic aerosols that reach Talos Dome (Becagli et al., 2004). In the same figure, raw data and a one-year running mean profile of MSA concentrations from the TD96 firn core were plotted. A point-to-point comparison between the MSA profile and sea ice extension anomalies does not demonstrate good agreement, despite positive sea ice anomalies usually coinciding with MSA spikes. In particular, the large sea ice positive anomalies recorded in the Ross Sea Sector from 1974 to 1976 are coincident with the large peak in the TD96 MSA profile and the sharp MSA spike starting in 1989 could correspond to the positive anomaly in the Ross Sea sea ice extension that occurred from 1988 to 1989. In the Wilkes Land sector, sea ice anomalies have lower amplitude than those recorded in the Ross Sea, probably because of the smaller extent of large embayment areas. The only large positive sea ice extension anomaly (1982–1984) in the entire Wilkes Land Sector record matches a slight MSA peak. This evidence shows that the TD96 MSA record mirrors the positive

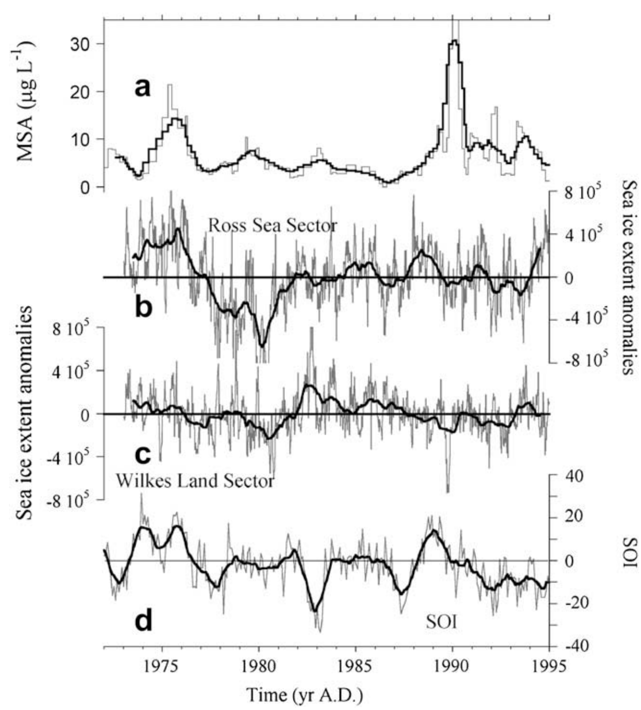

Fig. 3. MSA (plot a). Sea ice extension anomalies in the Ross Sea sector (plot b) and Pacific Oceanic sector facing Wilkes Land (plot c), and the SOI (plot d) temporal profile for the 1972–1996 time period. The one-year running mean profiles are shown as bold dark line in each plot.

anomalies of sea ice extension in the Ross Sea Sector. On the contrary, negative anomalies in the Ross Sea or Wilkes Land sectors seem not to be present in the TD96 MSA stratigraphy. As a consequence, with the exclusion of few large positive anomalies, a linear correlation between the TD96 MSA record and sea ice extent in the surrounding oceanic sectors is hard to find, which makes it necessary to apply a robust statistical approach, such as spectral analysis, to assess a significant relationship. Such statistical tools need extensive data to increase the results' significance. Unfortunately, reliable instrumental (satellite measurements) records of sea ice extent are only available since 1972 and the highest useful resolution is one year, which is imposed by MSA stratigraphy. Because of this, only 25 data points (from 1972 to 1996) for each series are available, which is not enough to give highly significant results. Therefore, we have to find another climatic parameter that is related to changes in sea ice extent whose record is available over a longer period. The key point of this approach is the teleconnection between sea ice extent and the atmospheric circulation modes around Antarctica (SOI and SAM) (Kwok and Comiso, 2002; Lefebvre et al., 2004). Indeed, the two positive anomalies in the Ross Sea Sector coinciding with a peak in the MSA profile are also related to positive values of the SOI (plot d in Fig. 3) suggesting a possible link between the SOI and MSA that requires a statistical approach on a more extensive data set.

3.2. Hemispheric and regional circulation modes

The link between the SOI and MSA stratigraphy from the ice core was first hypothesised by Legrand and Feniet-Saigne (1991). Due to strong interest in reconstructing past Southern Ocean climatic variability, further investigation has been carried out by several authors (e.g. Meyerson et al., 2002; Fundel et al., 2006) demonstrating that the link is different as a function of the area studied and more sites are required to understand this complex scenario.

In order to investigate the influence of the southern hemisphere circulation modes on the MSA ice core stratigraphy, it is useful to identify common periodical variation. The MSA, SOI and SAM spectral analysis plots are shown in Fig. 4(a–c). The MSA periodogram (Fig. 4(a)) shows four highly significant (with a confidence level >99%) periodicities of approximately 6.9, 4.9, 3.5 and 2.9 years. Three of them (6.9, 3.5, 2.9 years) are also present in the SOI power spectral plot with a confidence level >99% (Fig. 4(b)). The SAM periodogram demonstrates two dominant periodicities of 3.8 and 3.3 years (Fig. 4(c)), which could be related to the 3.5 year periodicity present in the MSA and SOI records as well as a complex family of peaks around 6.9 year periodicity that have a lower significance. Similar periodicities (2.2, 2.9, 3.5, 4.4, 5.5, 10.5 and 16.7 years) were found in the 20th century in the ACW variability by White and Tourre (2003). This evidence suggests that MSA deposition at Talos Dome is affected by atmospheric processes controlling the climate around Antarctica.

In order to understand the physical processes that lead to the observed common periodicities in the MSA, SOI and SAM, a cross-spectral analysis was carried out on the data sets. This statistical approach aims to assess the sign (positive or negative) of the correlation, the coherency (i.e. the goodness of the correlation between two periodical functions), and the phase relationship, which contains information about the synchronicity or temporal shift between the periodical oscillation of the two functions, of each common periodicity found in the time series of the two variables. In this work, we will discuss the periodicities of 6.9, 3.5, and 2.9 years identified both in the MSA and SOI periodograms and the common periodicities of 6.9 and 3.5 years found in the MSA and SAM spectral analysis. Cross-correlation plots are shown in Fig. 5(a) (MSA–SOI) and Fig. 5(b) (MSA–SAM). In the cross-spectral analysis, the SOI and

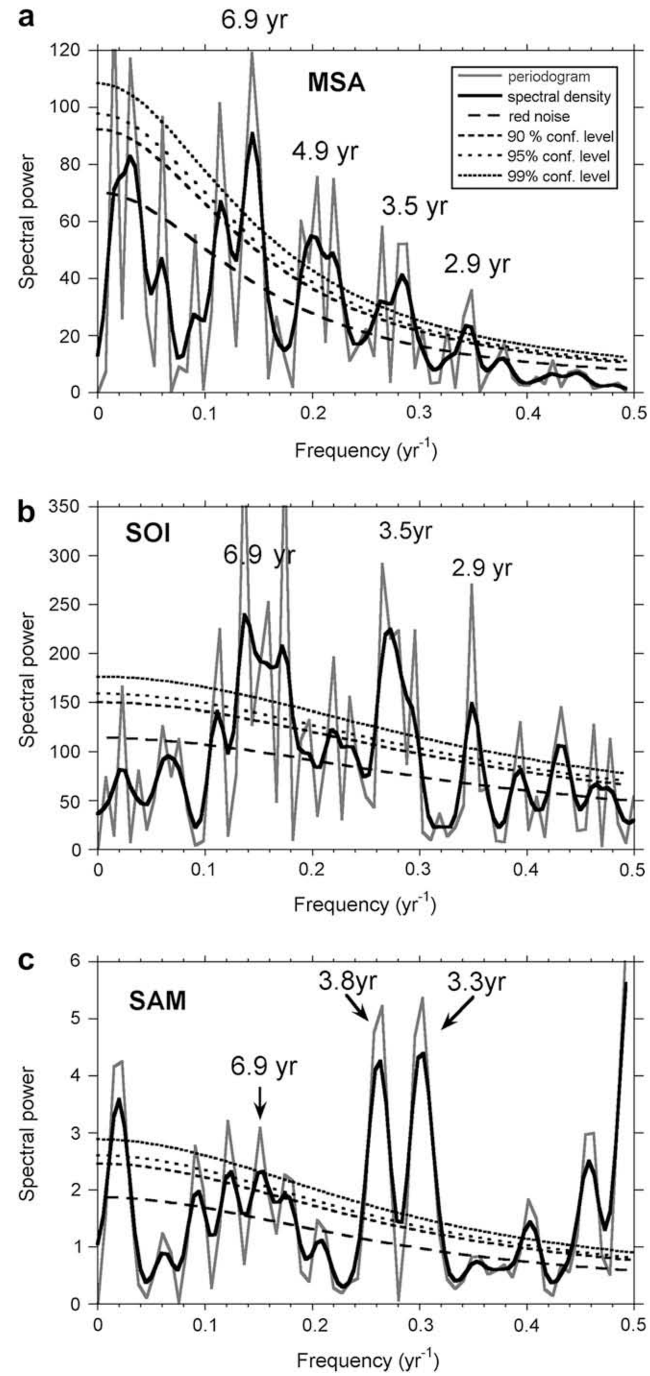

Fig. 4. MSA, SOI and SAM periodogram plots. Spectral analysis was performed using STATISTICA® software. The spectral density (bold dark line in the plots) was computed by the Tukey–Hamming (Blackman and Tukey, 1958) weighted moving average of the periodogram values (grey line). The red noise function and 90%, 95%, and 99% confidence levels are reported as dashed lines in each plot.

SAM are considered independent variables and MSA is the dependent variable. In this way, positive (negative) phases indicate that MSA variations lead (follow) SOI or SAM changes.

The highly significant 6.9 year periodicity found in both the MSA and SOI records (Fig. 5(a)) shows a large positive value in the MSA–SOI cross-spectral density plot, which indicates a positive correlation between MSA and the SOI (i.e. high SOI values correspond to high values of MSA) with a significant coherency (higher than 0.8) and no time shift between the two variations (phase approximately zero). A similar pattern can be observed, with a lower coherency, for the 2.9 year periodicity. Based on the close positive relationship

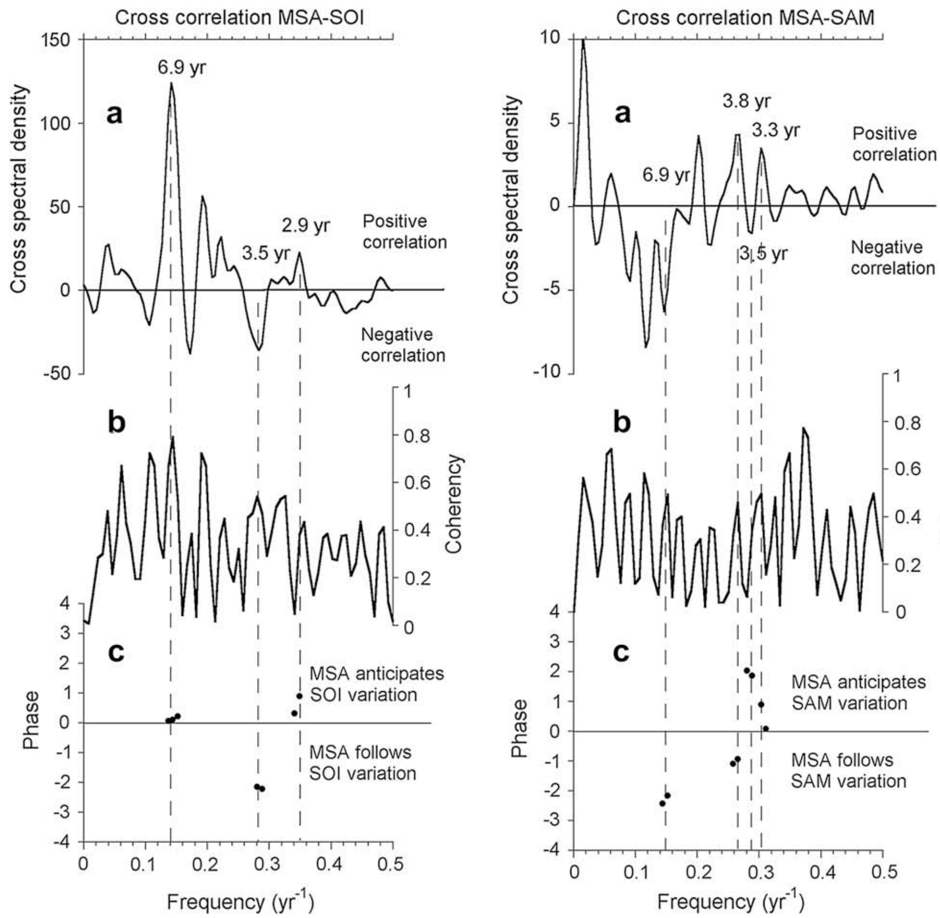

Fig. 5. MSA–SOI (plots on the left) and MSA–SAM (plots in the right) cross-spectral density, coherency, and phase plots. The SOI and SAM variables represent the independent parameter with respect to MSA. Cross-spectral analyses, coherency, and phase were computed using STATISTICA® software.

between sea ice in the Ross Sea and the SOI found by Kwok and Comiso (2002), we can explain this evidence by the relationship between sea ice extension and MSA. The effects of meteorological conditions that affect or are affected by increased sea ice extension and influence MSA transport processes toward coastal sites play a key role in fixing the positive or negative correlation. For instance, Abram et al. (2007) found a negative relationship between MSA in three sites around the Weddell Sea and winter sea ice in the Northern Weddell Sea over an interannual (about a 7 year period) and a multidecadal (about a 20 year period) timescale. This negative relationship is likely due to variations in the strength of cold offshore wind that acts to synergistically increase sea ice extension while decreasing MSA delivery to the ice core sites.

With regard to the area of interest, several studies (e.g. Bertler et al., 2006) report that the SOI has a fundamental effect on the position of low-pressure fields around Antarctica, especially the Amundsen Sea low-pressure (Amundsen Sea Low – L_{AS}). During La Niña events (SOI >1), the formation of a strong L_{AS} centred on the Ross Sea basin is favoured that, in turn, enhances the low-level easterly jet and encourages katabatic flow from the Antarctic continent. At higher atmospheric levels, a fast advection of air masses from the sea delivers moisture and marine (biogenic and sea spray) aerosol from the Ross Sea to the Talos Dome area and closes the atmospheric circulation cell (see Fig. 3 in Bertler et al., 2006). In this scenario, the positive correlation between MSA at Talos Dome and the SOI at 6.9 and 2.9 years is stronger because of both source intensity and transport efficiency.

For the 6.9 year periodicity, the MSA–SAM cross-spectral density shows a negative value, which indicates that maximum MSA concentrations in the Talos Dome snow deposition correspond to the SAM negative values. The coherency is lower than those observed for the MSA–SOI cross correlation and a negative phase value shows that MSA changes follow about one year after the SAM variations. On the other hand, the 2.9 year periodicity is not present in the SAM spectral power plot (Fig. 4(c)). This evidence implies that, for the 6.9 and 2.9 year periodicities, the increase in MSA concentration in snow layers at Talos Dome are only driven by synchronous SOI oscillation.

A different conclusion could be drawn for the periodicities in the range of 3.8–3.3 years. Fig. 5(a) and (b) shows a negative correlation both for the MSA–SOI and the MSA–SAM relationships at a 3.5 year periodicity, but coherency plots show that the MSA–SAM relationship is not significant and the MSA–SOI phase plot indicates that MSA variations are recorded about one year later than SOI changes. In this case, the delay in the MSA variation compared with the SOI oscillation and the negative correlation is hard to explain. On the contrary, periodicities at 3.3 and 3.8 years reveal a positive correlation between MSA and SAM with a time shift of less than one year (low phase values), but are not significantly identified in the MSA–SOI cross-spectral density plot. In this way, the effect of SAM on MSA at Talos Dome is dominant in this frequency range. Lefebvre et al. (2004) reported large sea ice extent in the Ross Sea when SAM positive values occurred, therefore the correlation between the SAM and MSA at Talos Dome could occur through sea ice extent in the Ross Sea. Thompson and Solomon (2002) suggested that positive SAM anomalies favour colder temperatures around Antarctica, which are associated to an increased continent insulation caused by a strengthening of the polar vortex. The effect of SAM on MSA deposition at Talos Dome is more complex for the range of the 3.3–3.8 year periodicity than that previously observed for SOI with a 6.9 year periodicity. Colder conditions allow for the formation of more sea ice while a more intense polar vortex creates a less efficient transport mechanism for marine air masses from coastal to inner areas of Antarctica. The prevalence of one of these factors (source intensity or transport efficiency) could determine the deposition of MSA at Talos Dome. Therefore, the positive relationship between SAM and MSA could occur via sea ice extension, but, since there is no transport efficiency increases as sea ice extension increases, the link SAM–MSA is less univocal (frequency split and low coherency) than SOI–MSA (same frequency, high coherency).

4. Conclusions

This work contributes to the understanding of variation in MSA concentration in an ice core drilled during the 1996–1997 summer Antarctic Campaign at the coastal plateau site of Talos Dome.

The complex role of changes in source intensity (changes in sea ice cover) and transport processes is the major reason for the difficulty in directly correlating the MSA profile and the Ross Sea ice record. Spectral analysis on MSA for the previous 140 years covered by the firn core (1860–1996) and climatic parameters suggest that there is a link between periodical variations of the SOI, SAM, ACW and MSA at Talos Dome.

In this work, we try to explain the periodicity of 6.9, 3.5 and 2.9 years found in the MSA profile as a function of the SOI and SAM variability. The periodicities of 2.9 years and, more significantly, 6.9 years are mainly related to the Ross Sea climate variability due to the SOI oscillation. MSA periodical oscillation demonstrates a strong positive correlation for these periodicities and is synchronous with corresponding SOI periodicity. These periodicities could be related to an increase in MSA source intensity caused by increased DMS production from phytoplanktonic activity, which is, in turn, related to the sea ice extent in the Ross Sea area as well as an increase in the strength of transport processes. Both of these factors are correlated with the SOI positive values (La Niña events). On the contrary, the MSA periodicity 3.5 years is primarily related to the SAM variability as a result of two periodicities (3.3 and 3.8 years). Furthermore, positive SAM values are related to an increased sea ice extent in the Ross Sea sector, but this condition also increases the strength of the polar vortex, which reduces the transport process intensity and decreases the delivery of air masses enriched with MSA from oceanic areas to Talos Dome. Therefore, the SAM positive values on MSA concentrations in the snow layers at Talos Dome are less effective than the ones SOI positive, which are the effect of increased source intensity and an increase in transport processes.

Finally, MSA deposition at Talos Dome not only responds to a greater sea ice extension in the Ross Sea, but also to transport processes from oceanic areas toward Talos Dome. When source intensity and transport efficiency increase contemporaneously, their effect on MSA deposition at Talos Dome is univocal. These processes occur primarily with a periodicity of 6.9 years over the previous 140 years.

Acknowledgements

This research was funded by the MIUR-PNRA program through a cooperation agreement among the PNRA consortium, Milano-Bicocca University, and Venice University in the framework of the "Glaciology" and "Chemistry of Polar Environments" projects. This work is an Italian contribution to the ITASE project.

References

Abram, N.J., Mulvaney, R., Wolff, E.W., Mudelsee, M., 2007. Ice core records as sea ice proxies: an evaluation from the Weddell Sea region of Antarctica. J. Geophys. Res. 112, D15101. doi:10.1029/2006JD008139.

Andreae, M.O., Crutzen, P.J., 1997. Atmospheric aerosols: biogeochemical sources and role in atmospheric chemistry. Science 276, 1052–1058. doi:10.1126/science.276.5315.1052.

de Angelis, M., Legrand, M., 1995. Preliminary investigations of post depositional effects on HCl, HNO_3, and organic acids in polar firn layers. In: Delmas, R.J. (Ed.), Ice Core Studies of Global Biogeochemical Cycles. NATO ASI Series, Series I, vol. 30. Springer, New York, pp. 361–381.

Becagli, S., Benassai, S., Castellano, E., Largiuni, O., Migliori, A., Traversi, R., Udisti, R., 2004. Chemical characterization of the last 250 years of snow deposition at Talos Dome. Int. J. Environ. Anal. Chem. 84 (6–7), 523–536.

Benassai, S., Becagli, S., Gragnani, R., Magand, O., Proposito, M., Fattori, I., Traversi, R., Udisti, R., 2005. Sea spray deposition in Antarctic coastal and plateau areas from ITASE traverses. Ann. Glaciol. 41, 32–40.

Bertler, N.A.N., Naish, T.R., Mayewski, P.A., Barrett, P.J., 2006. Opposing oceanic and atmospheric ENSO influences on the Ross Sea Region, Antarctica. Adv. Geosci. 6, 83–86. SRef-ID: 1680-7359/adgeo/2006-6-83.

Blackman, R.B., Tukey, J., 1958. The Measurement of Power Spectral From the Point of View of Communication Engineering. Dover, New York.

Brimblecombe, P., 1996. Air Composition and Chemistry. Cambridge University Press.

Charlson, R., Lovelock, J.E., Andreae, M.O., Warren, S.G., 1987. Oceanic phytoplankton, atmospheric sulphur, cloud albedo and climate. Nature 326 (6114), 655–661.

Curran, M.A., Palmer, A.S., Van Ommen, T.D., Morgan, V.I., Phillips, K.L., McMorrow, A.J., Mayewski, P.A., 2002. Post-depositional movement of methanesulphonic acid at Law Dome, Antarctica, and the influence of accumulation rate. Ann. Glaciol. 35, 333–339.

Curran, M.A., Palmer, A.S., Van Ommen, T.D., Morgan, V.I., Phillips, K.L., Palmer, A.S., 2003. Ice core evidence for Antarctic sea ice decline since the 1950s. Science 302, 1203–1206.

Frezzotti, M., Bitelli, G., De Michelis, P., Deponti, A., Forieri, A., Gandolfi, S., Maggi, V., Mancini, F., Remy, F., Tabacco, I.E., Urbini, S., Vittuari, L., Zirizzotti, A., 2004. Geophysical survey at Talos Dome, East Antartica: the search for a new deep-drilling site. Ann. Glaciol. 39, 423–432.

Fundel, F., Fischer, H., Weller, R., Traufetter, F., Oerter, H., Miller, H., 2006. Influence of large-scale teleconnection patterns on methane sulfonate ice core records in Dronning Maud Land. J. Geophys. Res. 111, D04103. doi:10.1029/2005JD005872.

Gabric, A.J., Shephard, J.M., Knight, J.M., Jones, G., Trevena, A.J., 2005. Correlations between the satellite-derived seasonal cycles of phytoplankton biomass and aerosol optical depth in the Southern Ocean: evidence for the influence of sea ice. Global Biogeochem. Cycles 19, GB4018. doi:10.1029/2005GB002546.

Ghil, M., Allen, M.R., Dettinger, M.D., Ide, K., Kondrashov, D., Mann, M.E., Robertson, A.W., Saunders, A., Tian, Y., Varadi, F., Yiou, P., 2002. Advanced spectral methods for climatic time series. Rev. Geophys. 40, 1-1–1-41. doi:10.1029/2001RG000092.

Gondwe, M., Krol, M., Gieskes, W., Klaassen, W., de Baar, H., 2003. The contribution of ocean-leaving DMS to the global atmospheric burdens of DMS, MSA, SO_2, and $nssSO_4^{2-}$. Global Biogeochem. Cycles 17 (2), 1056. doi:10.1029/2002GB001937.

Hall, A., Visbeck, M., 2002. Synchronous variability in the southern hemisphere atmosphere, sea ice and ocean resulting from the Annular Mode. J. Clim. 15, 3043–3057.

Hasselmann, K., 1976. Stochastic climate models. Tellus 6, 473–485.

Keeling, R., Stephens, B., 2001. Antarctic sea ice and the control of Pleistocene climate instability. Paleoceanography 16 (1), 112–131.

Kwok, R., Comiso, J.C., 2002. Southern Ocean climate and sea ice anomalies associated with the Southern Oscillation. J. Clim. 15, 487–501.

Lefebvre, W., Goosse, H., Timmermann, R., Fichefet, T., 2004. Influence of the Southern Annular Mode on the sea ice–ocean system. J. Geophys. Res. 109, C09005. doi:10.1029/2004JC002403.

Legrand, M., Feniet-Saigne, C., Saltzman, E.S., Germanin, C., Barkov, N.I., Petrov, V.N., 1991. Ice-core record of oceanic emissions of dimethylsulphide during the last climate cycle. Nature 350, 144–146.

Legrand, M., Hammer, C., De Angelis, M., Savarino, J., Delmas, R., Clausen, H., Johnsen, S.J., 1997. Sulfur-containing species (methanesulfonate and SO_4) over the last climatic cycle in the Greenland Ice Core Project (central Greenland) ice core. J. Geophys. Res. 102 (C12), 26,663–26,679.

Legrand, M., Leopold, A., Dominee, F., 1996. Acidic gases (HCl, HF, HNO_3, HCOOH, and CH_3COOH): a review of ice core data and some preliminary discussions on their air–snow relationships. In: Wolff, E.W., Bales, R.C. (Eds.), Processes of Chemical Exchange Between the Atmosphere and Polar Snow. NATO ASI Series, Series I, vol. 43. Springer, New York, pp. 19–43.

Legrand, M., Feniet-Saigne, C., 1991. Methanesulfonic acid in south polar snow layers. A record of strong El Niño? Geophys. Res. Lett. 18 (2), 187–190.

Malin, G., Turner, S.M., Liss, P.S., 1992. Sulfur: the plankton/climate connection. J. Phycol. 28, 590–597.

Mann, M.E., Lees, J.M., 1996. Robust estimation of background noise and signal detection on climate time series. Clim. Change 33, 409–445.

Meskhidze, N., Nenes, A., 2006. Phytoplankton and cloudiness in the Southern Ocean. Science 314 (5804), 1419–1423. doi:10.1126/science.1131779.

Meyerson, E.A., Mayewski, P.A., Kreutz, K.J., Meeker, D.L., Whitlow, S.I., Twickler, M.S., 2002. The polar expression of ENSO and sea-ice variability as recorded in a South Pole ice core. Ann. Glaciol. 35, 430–436.

Mitchell, J.M., 1976. An overview of climatic variability and its causal mechanisms. Quat. Res. 6, 481–493.

Morganti, A., Becagli, S., Castellano, E., Severi, M., Traversi, R., Udisti, R., 2007. An improved flow analysis–ion chromatography method for determination of cationic and anionic species at trace levels in Antarctic ice cores. Anal. Chim. Acta 603, 190–198.

O'Dwyer, J., Isaksson, E., Vinje, T., Jauhiainen, T., Moore, J., Pohjola, V., Vaikmäe, R., van de Wal, R.S., 2000. Methanesulphonic acid in a Svalbard ice core as an indicator of ocean climate. Geophys. Res. Lett. 27 (8), 1159–1162.

Pasteur, E.C., Mulvaney, R., 2000. Migration of methanesulphonate in Antarctic firn and ice. J. Geophys. Res. 105 (D9), 11,525–11,534.

Pasteur, E.C., Mulvaney, R., Peel, D.A., Saltzman, E.S., Whung, P.-J., 1995. A 340-year record of biogenic sulphur from Weddel Sea area, Antarctica. Ann. Glaciol. 21, 169–174.

Rankin, A.M., Wolff, E.W., Martin, S., 2002. Frost flowers: implications for tropospheric chemistry and ice core interpretation. J. Geophys. Res. 107 (D23), 4683. doi:10.1029/2002JD002492.

Röthlisberger, R., Bigler, M., Wolff, E.W., Joos, F., Monnin, E., Hutterli, M.A., 2004. Ice core evidence for the extent of past atmospheric CO_2 change due to iron fertilisation. Geophys. Res. Lett. 31, L16207. doi:10.1029/2004GL020338.

Saigne, C., Legrand, M., 1987. Methanesulfonic acid in Antarctic ice. Nature 330, 240–242.

Sedwick, P.N., DiTullio, G., 1997. Regulation of algal blooms in Antarctic shelf waters by the relase of iron from melting sea ice. Geophys. Res. Lett. 24 (20), 2515–2518.

Stefels, J., 2000. Physiological aspects of the production and conversion of DMSP in marine algae and higher plants. J. Sea Res. 43, 183–197. doi:10.1016/S1385-1101(00)00030-7.

Stenni, B., Proposito, M., Gragnani, R., Flora, O., Jouzel, J., Falourd, S., Frezzotti, M., 2002. Eight centuries of volcanic signal and climate change at Talos Dome (East Antarctica). J. Geophys. Res. 107 (D9). doi:10.1029/2000JD000317.

Stephens, B.B., Keeling, R.F., 2000. The influence of Antarctic sea ice on glacial–interglacial CO_2 variation. Nature 404, 171–174.

Thompson, D.W.J., Solomon, S., 2002. Interpretation of recent Southern Hemisphere climate change. Science 296, 895–899.

Turner, J., 2004. Review: the El Niño – Southern Oscillation and Antarctica. Int. J. Clim. 24, 1–31.

Vairavamurthy, A., Andreae, M.O., Iverson, R.L., 1985. Biosynthesis of dimethylsulfide and dimethylpropiothetin by *Hymenomonas carterae* in relation to sulfur source and salinity variations. Limnol. Oceanogr. 30, 59–70.

Wagnon, P., Delmas, R.J., Legrand, M., 1999. Loss of volatile acid species from upper firn layers at Vostok, Antarctica. J. Geophys. Res. 104, 3423–3431. doi:10.1029/98JD02855.

Welch, K.A., Mayewski, P.A., Whitlow, S.I., 1993. Methanesulphonic acid in coastal Antarctic snow related to sea-ice extent. Geophys. Res. Lett. 20 (6), 443–446.

White, W.B., Tourre, Y.M., 2003. Global SST/SLP waves during the 20th century. Geophys. Res. Lett. 30 (12), 1651. doi:10.1029/2003GL017055.

Whung, P.-Y., Saltzman, E.S., Spencer, M.J., Mayewski, P., Gundestrup, N., 1994. A two hundred year record of biogenic sulfur in a South Greenland ice core (20D). J. Geophys. Res. 99, 1147–1156.

Wolff, E.W., Fischer, H., Fundel, F., Ruth, U., Twarloh, B., Littot, G.C., Mulvaney, R., Röthlisberger, R., de Angelis, M., Boutron, C.F., Hansson, M., Jonsell, U., Hutterli, M.A., Lambert, F., Kaufmann, P., Stauffer, B., Stocker, T.F., Steffensen, J.P., Bigler, M., Siggaard-Andersen, M.L., Udisti, R., Becagli, S., Castellano, E., Severi, M., Wagenbach, D., Barbante, C., Gabrielli, P., Gaspari, V., 2006. Southern Ocean sea-ice extent, productivity and iron flux over the past eight glacial cycles. Nature 440. doi:10.1038/nature04614.